Journal of King Saud University - Science 36 (2024) 103273

Contents lists available at ScienceDirect

Journal of King Saud University - Science

journal homepage: www.sciencedirect.com

Full Length Article

Control of conjunctivitis virus with and without treatment measures: A bifurcation analysis

Muhammad Owais Kulachi [a], Aqeel Ahmad [a,b], Evren Hincal [b,c], Ali Hasan Ali [d,e,f,g,*], Muhammad Farman [h,i], Muhammad Taimoor [a]

[a] Department of Mathematics, Ghazi University D G Khan 32200, Pakistan
[b] Mathematics Research Center, Near East University, Near East Boulevard, Nicosia North Cyprus, 99138, Cyprus
[c] Department of Mathematics, Near East University, Near East Boulevard, Nicosia North Cyprus, 99138, Cyprus
[d] Department of Mathematics, College of Education for Pure Sciences, University of Basrah, 61001, Basrah, Iraq
[e] Institute of Mathematics, University of Debrecen, Pf.400, H-4002, Debrecen, Hungary
[f] Technical Engineering College, Al-Ayen University, 64001, Dhi Qar, Iraq
[g] Department of Business Management, Al-imam University College, 34011, Balad, Iraq
[h] Faculty of Art and Science, University of Kyrenia, Kyrenia, TRNC, Mersin 10, Turkey
[i] Department of Computer Science and Mathematics, Lebanese American University, Beirut, Lebanon

ARTICLE INFO

Keywords:
Mathematical modeling
Boundedness
Uniqueness
Reproductive number "R_0"
Flip bifurcation
Atangana–Toufik

ABSTRACT

This study aims to examine the early detection and treatment of conjunctivitis (eye infection) through vaccination and recovery measures, both with and without medication. We develop an immune system-boosting mathematical model and convert it to a fractionally ordered model using the ABC operator. Key properties, such as the uniqueness and boundedness of the model, are investigated using Banach space. To assess the stability of the newly developed $SEVIR_uR_i$ system and confirm the occurrence of flip bifurcation, we conduct both qualitative and quantitative analyses. We calculate the basic reproductive number, R_0, using an advanced approach and analyze its impact across different sub-compartments. Sensitivity analysis is performed on each parameter to understand the rate of change sensitivity. The Atangana–Toufik method is employed to solve the system for various fractional values, providing a reliable bounded solution. Simulations are conducted to observe the real behavior and effects of the conjunctivitis virus, showing that individuals with a strong immune system can recover with or without medication. Finally, we determine the actual state of virus control post-early detection, accounting for treated and untreated individuals due to the robust immune system and precautionary measures.

1. Introduction

In the 13th century, Fibonacci introduced the famous Fibonacci sequence to describe population growth, marking the beginning of mathematics in biology. Later, Daniel Bernoulli used mathematical concepts to explain microscopic organisms' forms, and Johannes Reinke coined the term "bio math" in 1901. Essentially, bio math involves the theoretical study of mathematical models to understand the principles underlying biological systems' structure and function.

The last few decades have seen significant advancements in the biological sciences, driven by technological progress. Mathematics has consistently contributed to society, bringing substantial advancements to the natural sciences. Similarly, biological research can be revolutionized through mathematical models, which help unravel life's complexities. Modern computer algebra systems have simplified solving complex mathematical problems, enabling scientists to focus on understanding mathematical biology (Chou and Friedman, 2016; Yeargers et al., 2013).

Recent years have seen increased attention to the mathematical modeling of various biological, physical, and epibiological systems. This attention is due to mathematical models' ability to incorporate complex elements. Scholars have particularly focused on mathematical biology in areas such as infectious disease modeling, human anatomy growth, and body fluid dynamics. Mathematical models have provided frameworks to understand biological processes, determine threshold parameters, clarify transmission dynamics, and suggest effective control strategies for infectious diseases (Murray, 2003; Kyere et al., 2018).

* Corresponding author.
E-mail addresses: owaiskulachi1997@gmail.com (M.O. Kulachi), aqeelahmad.740@gmail.com (A. Ahmad), evren.hincal@neu.edu.tr (E. Hincal), ali.hasan@science.unideb.hu (A.H. Ali), farmanlink@gmail.com (M. Farman), kulachi114@gmail.com (M. Taimoor).

https://doi.org/10.1016/j.jksus.2024.103273
Received 30 January 2024; Received in revised form 17 May 2024; Accepted 25 May 2024
Available online 27 May 2024
1018-3647/© 2024 The Authors. Published by Elsevier B.V. on behalf of King Saud University. This is an open access article under the CC BY-NC-ND license (http://creativecommons.org/licenses/by-nc-nd/4.0/).

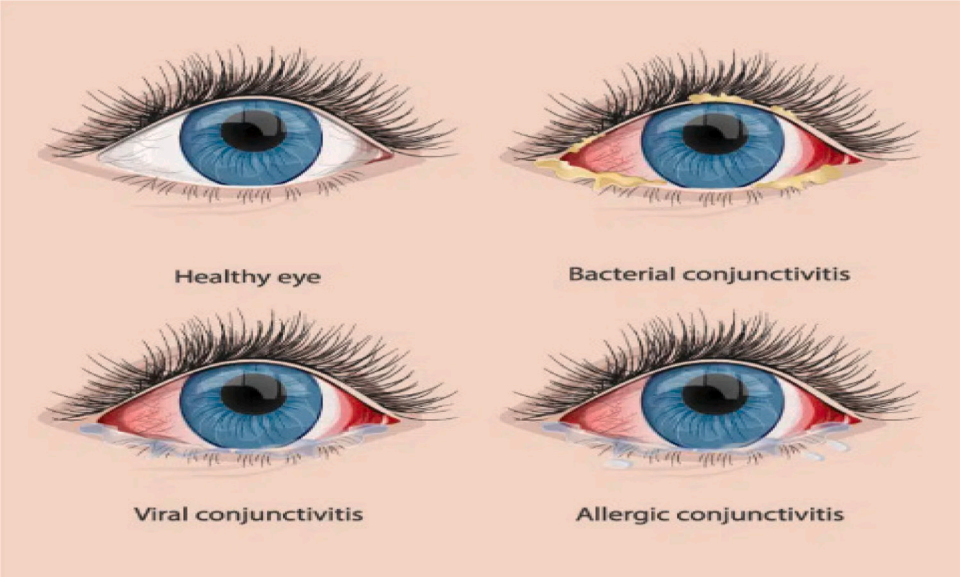

Fig. 1. Conjunctivitis (Pink Eye) symptoms.

Conjunctivitis, or pink eye, is a highly contagious condition caused by inflammation of the conjunctiva, triggered by bacterial, viral, or allergic infections. Various forms of conjunctivitis, such as allergic conjunctivitis, occur seasonally due to exposure to allergens like pollen, dust mites, animal dander, and contact lenses (Center for Disease Control (CDC), n.d.; Fehily et al., 2015). Transmission occurs through contact with infected individuals or contaminated objects. Acute Hemorrhagic Conjunctivitis (ADC) is a specific viral type with an incubation period of 1 to 3 days, presenting symptoms such as tearing, irritation, photophobia, sore throat, lid swelling, and purulent discharges (Elliot, 1925).

Infectious conjunctivitis, including bacterial, viral, and ophthalmia neonatorum, involves infection of the conjunctiva and sclera. Symptoms include itching, soreness, tearing, pus discharge, and light sensitivity. Effective control measures include antibiotic eye drops, hygiene practices, isolation, and allowing the disease to run its course, typically lasting 2 to 3 weeks. Conjunctivitis is more prevalent in tropical regions (Malu, 2014; Kimberlin, 2018). In Fig. 1, the physical symptoms of eyes infected by the conjunctivitis virus are illustrated.

Fractional calculus is widely used in scientific disciplines, especially physics and engineering. Fractional order models are preferred over traditional integer order models for their ability to account for genetic and memory aspects of systems (Ahmad et al., 2024; Alsaud et al., 2024). Examples include fractional models for lung cancer and coronavirus, demonstrating the influence of fractional-order derivatives on disease transmission. The COVID-19 pandemic highlighted the need for such models due to social and economic disruptions (Tomar and Chadha, 2023; Chadha et al., 2023). The Generalized Damped Forced Korteweg–de Vries (GDFKdV) equation and the Damped Forced Korteweg–de Vries (DFKdV) equation have also been used to study nonlinear wave propagation and reaction dynamics (Tomar et al., 2023). Models of some diseases can be studied in certain environments such as fuzzy environment to employ fuzzy parameters accounts for the variability in parameter values among individuals within the population (Dayan et al., 2023).

Conjunctivitis often manifests during the rainy season when humid conditions favor the virus's spread, particularly in tropical regions like Thailand Ghazali et al. (2003), Chansaenroj et al. (2015). Isolating infected individuals and granting sick leave for home isolation can accelerate recovery and reduce infectious interactions. The American Academy of Pediatrics recommends student isolation to prevent rapid transmission in schools (Chowell et al., 2006). Mathematical models of conjunctivitis have been developed to enhance understanding, with notable contributions from Suksawat and Naowarat (2014), Unyong and Naowarat (2014), Sangthongjeen et al. (2015), Alalhareth et al. (2023).

1.1. Basic definitions

Definition 1.1. Atangana–Baleanu's fractional-order derivative in the Liouville–Caputo sense (ABC) is defined by Atangana and Baleanu (2016)

$$ {}_0^{ABC}D_t^{\xi}\{g(t)\} = \frac{AB(\xi)}{n-\xi}\int_{\xi}^{t}\frac{d^n}{dw}g(w)E_{\xi}\left[-\xi\frac{(t-w)^{\xi}}{n-\xi}\right]dw, n-1<\xi<n, \quad (1) $$

where E_{ξ} represents the Mittag-Leffler function, $AB(\xi)$ represents a normalization function, and $AB(0) = AB(1) = 1$.

Definition 1.2. The Laplace transform of Eq. (1) is given by:

$$ [{}_0^{ABC}D_t^{\xi}g(t)]s = \frac{AB(\xi)}{1-\xi}\frac{s^{\xi}L[g(t)](s) - s^{\xi-1}g(0)}{s^{\xi}+\frac{\xi}{1-\xi}}. $$

Definition 1.3. The Sumudu transform (ST) of Eq. (1) is given by:

$$ ST\{{}_0^{ABC}D_t^{\xi}g(t)\}s = \frac{B(\xi)}{1-\xi}\left(\xi\Gamma(\xi+1)E_{\xi}\left(-\frac{1}{1-\xi}v^{\xi}\right)\right). $$

Definition 1.4. The fractional integral of order ξ for the Atangana–Baleanu function $g(t)$ is given by:

$$ {}_0^{ABC}I_t^{\xi}[g(t)] = \frac{1-(\xi)}{B-\xi}g(t) + \frac{(\xi)}{B(\xi)\Gamma(\xi)}\int_{\xi}^{t}g(s)(t-s)^{\xi-1}ds. $$

2. Formulation of SEVIR_u R_i model

Conjunctivitis as a bacterial disease with pink eyes is discussed in Sangsawang et al. (2012), along with its medication. We formulate a mathematical model for the conjunctivitis virus by introducing recovered individuals without medication. This new model, denoted SEVI$R_u R_i$, includes the following compartments: susceptible (S), exposed (E), vaccinated (V), infected (I), recovered without medication (R_u), and recovered with treatment (R_i). The key parameters in our model are:

- n: total population,

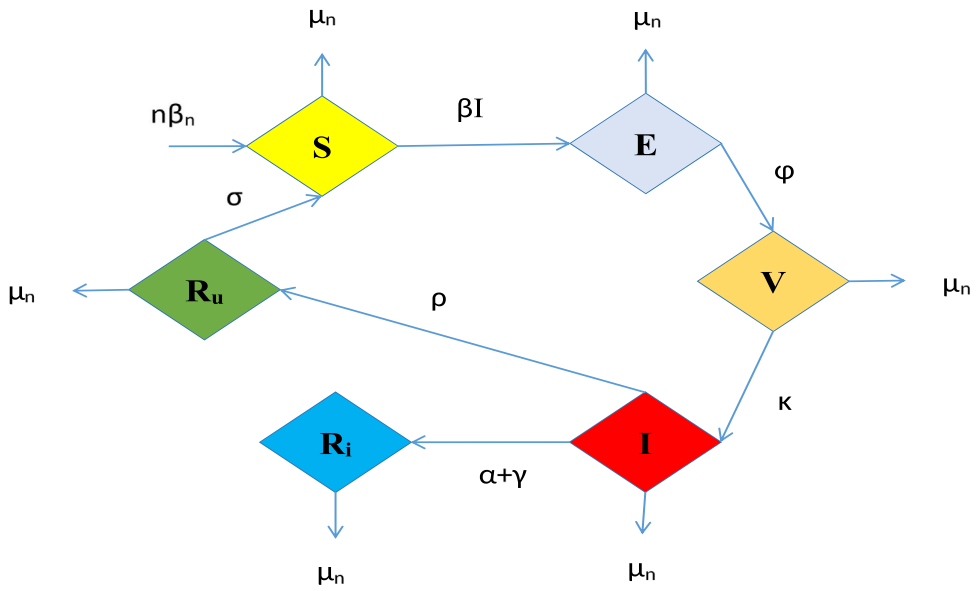

Fig. 2. The flowchart of the model formulation.

- β_n: birth rate,
- μ_n: death rate,
- β: transmission rate of Acute Hemorrhagic Conjunctivitis,
- ϕ: vaccination rate for uninfected individuals,
- κ: incubation rate for Acute Hemorrhagic Conjunctivitis,
- α: recovery rate with treatment,
- γ: recovery rate without medication,
- ρ: recovery rate without medication,
- σ: rate at which individuals become susceptible again.

The flowchart for the newly developed model SEVIR_u R_i is given in Fig. 2.

The developed model, derived from the flowchart and the generalized constructed hypothesis mentioned above, is as follows:

Using the Atangana–Baleanu (ABC) fractional operator, the model becomes

$$\begin{aligned}
{}^{ABC}_{0}D^{\xi}_{t}S(t) &= n\beta_n + \sigma R_u - \beta IS - \mu_n S,\\
{}^{ABC}_{0}D^{\xi}_{t}E(t) &= \beta IS - \phi E - \mu_n E,\\
{}^{ABC}_{0}D^{\xi}_{t}V(t) &= \phi E - \kappa V - \mu_n V,\\
{}^{ABC}_{0}D^{\xi}_{t}I(t) &= \kappa V - (\alpha+\gamma+\rho+\mu_n)I,\\
{}^{ABC}_{0}D^{\xi}_{t}R_u(t) &= \rho I - (\sigma+\mu_n)R_u,\\
{}^{ABC}_{0}D^{\xi}_{t}R_i(t) &= (\alpha+\gamma)I - \mu_n R_i.
\end{aligned} \tag{2}$$

Here, ${}^{ABC}_{0}D^{\xi}_{t}$ represents ABC derivatives, where $0 < \xi \leq 1$. The initial conditions associated with this model are:

$$S(0) = S^0,\ E(0) = E^0,\ V(0) = V^0,\ I(0) = I^0,\ R_u(0) = R_u^0,\ R_i(0) = R_i^0.$$

The parameters and their values involved in developed mathematical model are given in Table 1.

We employ the Sumudu transform on Eq. (2) and, after restructuring the system and applying the inverse Sumudu transform, we obtain:

$$S_{k+1}(t) = S_k(0) + ST^{-1}\left\{\frac{1-\xi}{B(\xi)\xi\Gamma(\xi+1)E_\xi\left(-\frac{1}{1-\xi}w^\xi\right)} \times ST\left[n\beta_n + \sigma R_u - \beta IS - \mu_n S\right]\right.,$$

$$E_{k+1}(t) = E_k(0) + ST^{-1}\left\{\frac{1-\xi}{B(\xi)\xi\Gamma(\xi+1)E_\xi\left(-\frac{1}{1-\xi}w^\xi\right)} \times ST\left[\beta IS - \phi E - \mu_n E\right]\right.,$$

$$V_{k+1}(t) = V_k(0) + ST^{-1}\left\{\frac{1-\xi}{B(\xi)\xi\Gamma(\xi+1)E_\xi\left(-\frac{1}{1-\xi}w^\xi\right)} \times ST\left[\phi E - \kappa V - \mu_n V\right]\right.,$$

$$I_{k+1}(t) = I_k(0) + ST^{-1}\left\{\frac{1-\xi}{B(\xi)\xi\Gamma(\xi+1)E_\xi\left(-\frac{1}{1-\xi}w^\xi\right)} \times ST\left[\kappa V - (\alpha+\gamma+\rho+\mu_n)I\right]\right., \tag{3}$$

$$R_{uk+1}(t) = R_{uk}(0) + ST^{-1}\left\{\frac{1-\xi}{B(\xi)\xi\Gamma(\xi+1)E_\xi\left(-\frac{1}{1-\xi}w^\xi\right)} \times ST\left[\rho I - (\sigma+\mu_n)R_u\right]\right.,$$

$$R_{ik+1}(t) = R_{ik}(0) + ST^{-1}\left\{\frac{1-\xi}{B(\xi)\xi\Gamma(\xi+1)E_\xi\left(-\frac{1}{1-\xi}w^\xi\right)} \times ST\left[(\alpha+\gamma)I - \mu_n R_i\right]\right..$$

The resultant solution of (3) is given as

$$S(t) = \lim_{k\to\infty} S_k(t), E(t) = \lim_{k\to\infty} E_k(t), V(t) = \lim_{k\to\infty} V_k(t),$$
$$I(t) = \lim_{k\to\infty} I_k(t), R_u(t) = \lim_{k\to\infty} R_{uk}(t), R_i(t) = \lim_{k\to\infty} R_{ik}(t).$$

Theorem 2.1. *Consider a Banach space $(Y, \|\cdot\|)$ and let M be a self-map of Y satisfying*

$$\|My - Mr\| \leq \xi\|y - r\|, \quad \forall y, r \in Y, \tag{4}$$

where $0 \leq \xi < 1$. Assume that M is Picard M-stable.

For Eq. (3), we obtain

$$\frac{1-\xi}{B(\xi)\xi\Gamma(\xi+1)E_\xi\left(-\frac{1}{1-\xi}w^\xi\right)}.$$

The above expression shows the Lagrange multiplier.

Proof. Self-map M is defined on Eq. (3). Using norm properties and the triangle inequality, we get

$$\begin{aligned}
\|M[s_k(t)] - M[S_j(t)]\| \leq \|s_k(t) - S_j(t)\| + ST^{-1}\left\{\frac{1-\xi}{B(\xi)\xi\Gamma(\xi+1)E_\xi\left(-\frac{1}{1-\xi}w^\xi\right)}\right.\\
\times ST\left[n\beta_n + \sigma(R_{u_k}(t) - R_{u_j}(t)) - \beta(I_k(t) - I_j(t))(S_k(t) - S_j(t))\right.\\
\left.\left.-\mu_n(S_k(t) - S_j(t))\right]\right\}.
\end{aligned}$$

Similarly, we get analogous results for $\|M[e_k(t)] - M[E_j(t)]\|$, $\|M[v_k(t)] - M[V_j(t)]\|$, $\|M[i_k(t)] - M[I_j(t)]\|$, $\|M[r_{u_k}(t)] - M[R_{u_j}(t)]\|$, and $\|M[r_{i_k}(t)] - M[R_{i_j}(t)]\|$.

M fulfills the conditions of Theorem 2.1. Therefore, M must be Picard M-stable.

Theorem 2.2. *The iteration approach is used to find a unique singular solution to Eq. (2).*

Table 1
Description of parameters.

Parameter	Representation	Estimated values	References
n	Describes the whole population	1	Sangsawang et al. (2012)
β_n	Represents the birth rate	0.00004215	Sangsawang et al. (2012)
σ	Rate at which individuals become susceptible	0.005	Assumed
β	Transmission rate for Acute Hemorrhagic Conjunctivitis	0.004	Sangsawang et al. (2012)
μ_n	Represents the death rate	0.00004215	Sangsawang et al. (2012)
ϕ	Rate of vaccination for uninfected individuals	0.3	Assumed
κ	Characterizes for Acute Hemorrhagic Conjunctivitis as incubation rate	0.04	Sangsawang et al. (2012)
α	Incidence rate for recovered with treatment measures	0.08	Sangsawang et al. (2012)
γ	Incidence rate for recovered individuals without medication	0.3	Sangsawang et al. (2012)
ρ	Recovery rate without medication	0.0000008	Assumed

Proof. Consider the Hilbert space $M = P^2\big((v,u)\times(0,r)\big)$. In this context, M denotes the set of measurable functions, P represents the projection operator, and $\big((v,u)\times(0,r)\big)$ is the Cartesian product of the intervals (v,u) and $(0,r)$.

$$h : (v,u)\times[0,T]\to\mathbb{R}, \quad \iiint gh\,dg\,dh < \infty.$$

Certain operators are taken into account:

$$\xi = (0,0,0,0,0,0), \quad \xi = \begin{cases} n\beta_n + \sigma R_u - \beta I S - \mu_n S, \\ \beta I S - \phi E - \mu_n E, \\ \phi E - \kappa V - \mu_n V, \\ \kappa V - (\alpha+\gamma+\rho+\mu_n)I, \\ \rho I - (\sigma+\mu_n)R_u, \\ (\alpha+\gamma)I - \mu_n R_i. \end{cases}$$

We demonstrate that the inner product of

$$\big(T(S_{a11}(t) - S_{a12}(t), E_{b21}(t) - E_{b22}(t), V_{f61}(t) - V_{f62}(t), I_{c31}(t) - I_{c32}(t), R_{ud41}(t) - R_{ud42}(t), R_{ie51}(t) - R_{ie52}(t)), (v_1, v_2, v_3, v_4, v_5)\big).$$

involving $(S_{a11}(t) - S_{a12}(t), E_{b21}(t) - E_{b22}(t), V_{f61}(t) - V_{f62}(t), I_{c31}(t) - I_{c32}(t), R_{ud41}(t) - R_{ud42}(t), R_{ie51}(t) - R_{ie52}(t))$ are the system's unique solutions.

Considering the inner function and the norm, for large numbers e_1, e_2, e_3, e_4, e_5, and e_6, both solutions converge to the exact solution. Using topological notions, we derive five small positive parameters $(\varepsilon_{e_1}, \varepsilon_{e_2}, \varepsilon_{e_3}, \varepsilon_{e_4}, \varepsilon_{e_5}, \varepsilon_{e_6})$ such that

$$\|v_1\|, \|v_2\|, \|v_3\|, \|v_4\|, \|v_5\|, \|v_6\| \neq 0;$$

$$\|S_{a11}(t) - S_{a12}(t)\|, \|E_{b21}(t) - E_{b22}(t)\|, \|V_{f61}(t) - V_{f62}(t)\|,$$
$$\|I_{c31}(t) - I_{c32}(t)\|, \|R_{ud41}(t) - R_{ud42}(t)\|, \|R_{ie51}(t) - R_{ie52}(t)\| \to 0;$$
$$S_{a11}(t) = S_{a12}(t), \quad E_{b21}(t) = E_{b22}(t), \quad V_{f61}(t) = V_{f62}(t),$$
$$I_{c31}(t) = I_{c32}(t), \quad R_{ud41}(t) = R_{ud42}(t), \quad R_{ie51}(t) = R_{ie52}(t).$$

This completes the proof of uniqueness.

3. Analysis of equilibrium points and reproductive number

In this section, we conduct a comprehensive analysis of equilibrium points. To determine these points, it is necessary to set the left-hand side of the system (2) to zero. The equilibrium point corresponding to the absence of disease in this model is:

$$D_1(S,E,V,I,R_u,R_i) = \left(\frac{n\beta_n}{\mu_n}, 0, 0, 0, 0, 0\right).$$

Furthermore, the equilibrium point associated with the endemic state, after substituting the parameter values given in Table 1 and using Mathematica for simplification, is given by:

$$D_2(S^*,E^*,V^*,I^*,R_u^*,R_i^*) = (95.1242, 0.127117, 0.952377, 0.100239, 0.0000159042, 903.696).$$

3.1. Reproduction number and its analysis

The Jacobian matrices F and V are analyzed at the disease-free equilibrium point D_1. In these matrices, the element at position (i,j) of matrix F denotes the rate at which a virus-infected individual in compartment j spreads to compartment i, while the element at (i,j) in matrix V indicates the progression of the disease within compartment i. To compute the reproduction number, the spectral radius of the matrix FV^{-1} at the disease-free equilibrium point is evaluated. This matrix, known as the Next Generation Matrix, is given by:

$$J_0 = \begin{pmatrix} -\mu_n & 0 & 0 & -\frac{\beta n \beta_n}{\mu_n} & \sigma & 0 \\ 0 & -(\mu_n+\phi) & 0 & \frac{\beta n \beta_n}{\mu_n} & 0 & 0 \\ 0 & \phi & -(\mu_n+\kappa) & 0 & 0 & 0 \\ 0 & 0 & \kappa & -(\mu_n+\alpha+\gamma+\rho) & 0 & 0 \\ 0 & 0 & 0 & \rho & -(\mu_n+\sigma) & 0 \\ 0 & 0 & 0 & \alpha+\gamma & 0 & -\mu_n \end{pmatrix}.$$

$$J_0 = F - V.$$

We use Eq. (1) to derive the vectors F and V in our model.
The resultant matrix K is given by

$$K = FV^{-1}.$$

The characteristic equation is

$$|K - \Lambda I| = 0.$$

Solving this determinant, we obtain the eigenvalues Λ. The principal eigenvalue from this characteristic equation is the reproduction number (R_0), which is given by:

$$R_0 = \frac{n\beta\kappa\phi\beta_n}{\mu_n(\alpha+\gamma+\rho+\mu_n)(\kappa+\mu_n)(\phi+\mu_n)}.$$

3.2. Sensitivity analysis

Sensitivity analysis determines how different factors affect a model's stability, especially with ambiguous data. It helps identify critical process factors. The sensitivity of R_0 is examined by computing the partial derivatives of the threshold with respect to relevant parameters.

The value of R_0 is sensitive to changes in parameters. Our analysis shows that $\mu_n, \alpha, \rho, \gamma$, and $n, \beta_n, \kappa, \beta, \phi$ show contraction and expansion, respectively. For effective infection control, prevention is advised over treatment. These indices help identify essential factors in defining the infection's propagation capacity, as depicted in Fig. 3.

4. Flip bifurcation analysis

From Ngoma et al. (2022), we observe that none of the eigenvalues equal 1 or -1, indicating that our model (2) may exhibit bifurcation if the constants are taken as:

$$(n, \beta_n, \sigma, \beta, \mu_n, \phi, \kappa, \alpha, \gamma, \rho).$$

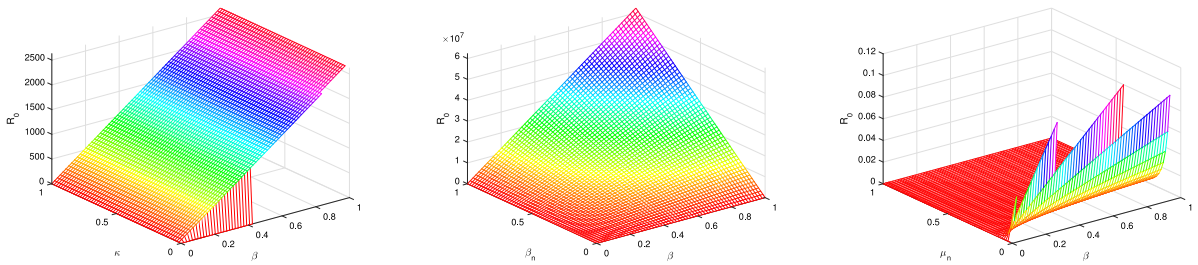

(a) $\mathbf{R}_0$ of β and κ (b) $\mathbf{R}_0$ of β and β_n (c) $\mathbf{R}_0$ of β and μ_n

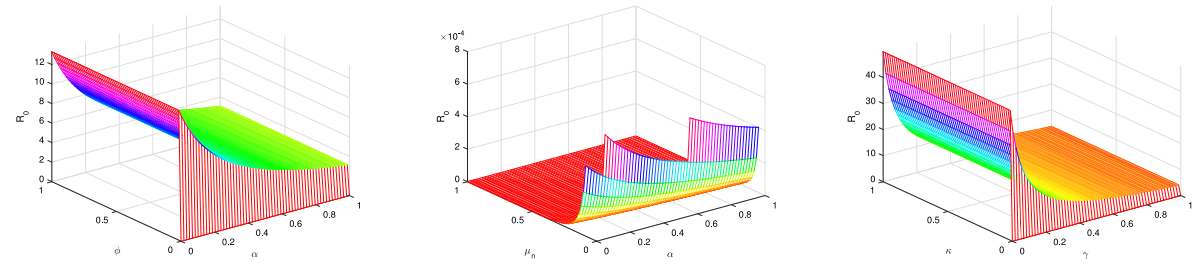

(d) $\mathbf{R}_0$ of α and ϕ (e) $\mathbf{R}_0$ of α and μ_n (f) $\mathbf{R}_0$ of γ and κ

Fig. 3. Reproductive number behavior for the newly developed system under different parameter effects.

This is given by:

$$F|_{E\left(\frac{n\beta_n}{\mu_n},0,0,0,0,0\right)} = \left\{(n,\beta_n,\sigma,\beta,\mu_n,\phi,\kappa,\alpha,\gamma,\rho) : \mu_n = 0\right\}.$$

We need to prove that bifurcation does not exist at

$$E\left(\frac{n\beta_n}{\mu_n},0,0,0,0,0\right),$$

if the constants are taken as:

$$(n,\beta_n,\sigma,\beta,\mu_n,\phi,\kappa,\alpha,\gamma,\rho) \in F|_{E\left(\frac{n\beta_n}{\mu_n},0,0,0,0,0\right)}.$$

Theorem 4.1. *Our model (2) does not have flip bifurcation at*

$$E\left(\frac{n\beta_n}{\mu_n},0,0,0,0,0\right),$$

if the constants are taken as:

$$(n,\beta_n,\sigma,\beta,\mu_n,\phi,\kappa,\alpha,\gamma,\rho) \in F|_{E\left(\frac{n\beta_n}{\mu_n},0,0,0,0,0\right)}.$$

Proof. Our model in Eq. (2) is invariant with respect to E, V, I, R_u and $R_i = 0$. To verify the bifurcation existence, we take E, V, I, R_u and $R_i = 0$. As a result:

$$S(t) = hn\beta_n + (1 - h\mu_n)S(t). \tag{5}$$

Applying Eq. (5), we get:

$$f(S(t)) = hn\beta_n + (1 - h\mu_n)S(t). \tag{6}$$

Now, if $\mu_n = 0$, $S(t) = \frac{n\beta_n}{\mu_n}$. Applying Eq. (6), we get:

$$\frac{\partial f(S(t))}{\partial S(t)}\Big|_{\mu_n=0, S(t)=\frac{n\beta_n}{\mu_n}} = 1. \tag{7}$$

Taking the partial derivative of $f(S(t))$ with respect to μ_n, and applying the values for $S(t)$ and μ_n, we get $-\frac{hn\beta_n}{\mu_n} \neq 0$. Then, applying the second partial derivative on Eq. (7), we get:

$$\frac{\partial^2 f(S(t))}{\partial S^2(t)} = 0. \tag{8}$$

This shows that our model in Eq. (2) does not exhibit bifurcation if the constants are taken as follows:

$$(n,\beta_n,\sigma,\beta,\mu_n,\phi,\kappa,\alpha,\gamma,\rho) \in F|_{E\left(\frac{n\beta_n}{\mu_n},0,0,0,0,0\right)}.$$

Using a combination of immune system impacts and therapy, we investigate a newly designed conjunctivitis virus model. The population is affected in a complex, time-dependent way; the interaction between conjunctivitis and this system is continuous.

The linearization technique is used to achieve the stability and boundedness of the model equations in Fig. 4. From the bifurcation diagrams, we infer that the model's behavior rises with control input and falls with extraction. The combination of medication and no medication creates a stable state for the conjunctivitis virus (pink eye) model. Fig. 4 supports our theoretical conclusions with time-stable graphs based on the parametric values.

5. Solutions by advanced numerical approach

We use an advanced numerical approach with a non-local, non-singular kernel for fractional differential equations to find reliable solutions. The system is given by:

$$\begin{cases} {}^{ABC}_{0}D S(t) = f_1(t, S(t), G(t)), \\ {}^{ABC}_{0}D E(t) = f_2(t, S(t), G(t)), \\ {}^{ABC}_{0}D V(t) = f_3(t, S(t), G(t)), \\ {}^{ABC}_{0}D I(t) = f_4(t, S(t), G(t)), \\ {}^{ABC}_{0}D R_u(t) = f_5(t, S(t), G(t)), \\ {}^{ABC}_{0}D R_i(t) = f_6(t, S(t), G(t)), \\ \text{where } G(t) = (E(t), V(t), I(t), R_u(t), R_i(t)). \\ S^0 = S_0, E^0 = E_0, V^0 = V_0, I^0 = I_0, R_u^0 = R_{u0}, R_i^0 = R_{i0}. \end{cases} \tag{9}$$

These equations can be converted to fractional integral equations using fractional calculus:

$$S(t) - S(0) = \frac{(1-\xi)}{ABC(\xi)} f_1(t, S(t), G(t)) + \frac{\xi}{ABC(\xi)\Gamma(\xi)} \int_0^t f_1(\sigma, S(\sigma), G(\sigma))(t-\sigma)^{\xi-1} d\sigma,$$

where $G(\sigma) = (E(\sigma), V(\sigma), I(\sigma), R_u(\sigma), R_i(\sigma))$.

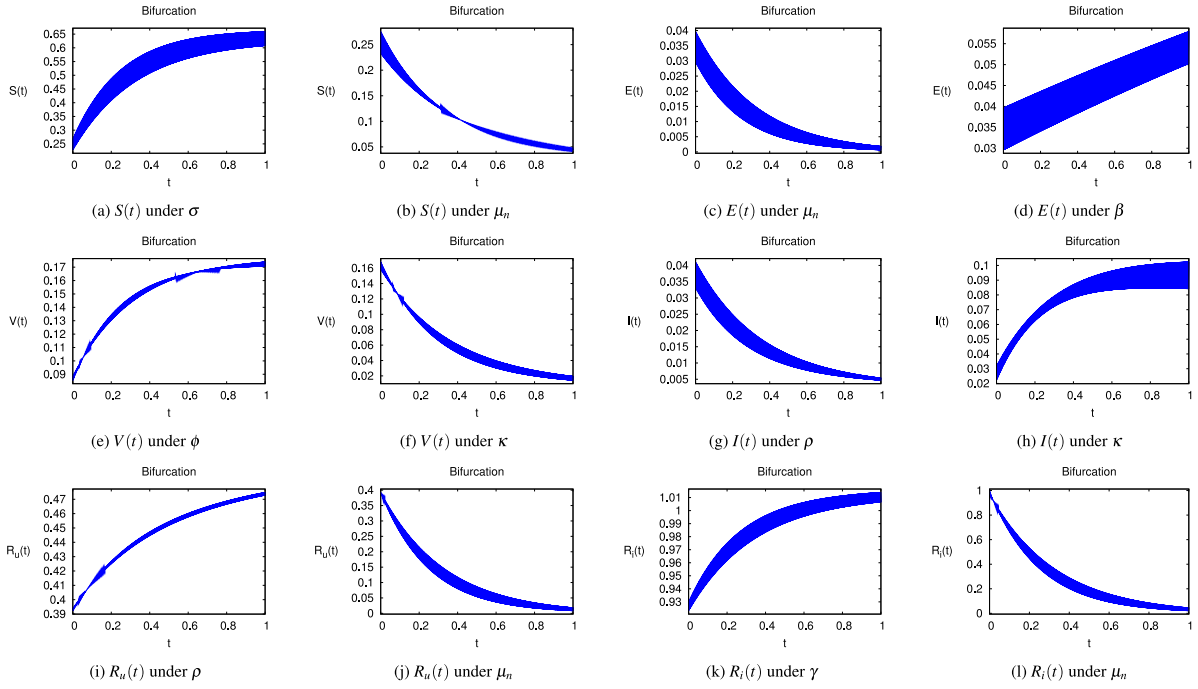

(a) $S(t)$ under σ (b) $S(t)$ under μ_n (c) $E(t)$ under μ_n (d) $E(t)$ under β

(e) $V(t)$ under ϕ (f) $V(t)$ under κ (g) $I(t)$ under ρ (h) $I(t)$ under κ

(i) $R_u(t)$ under ρ (j) $R_u(t)$ under μ_n (k) $R_i(t)$ under γ (l) $R_i(t)$ under μ_n

Fig. 4. Bifurcation analysis of continuous dynamics.

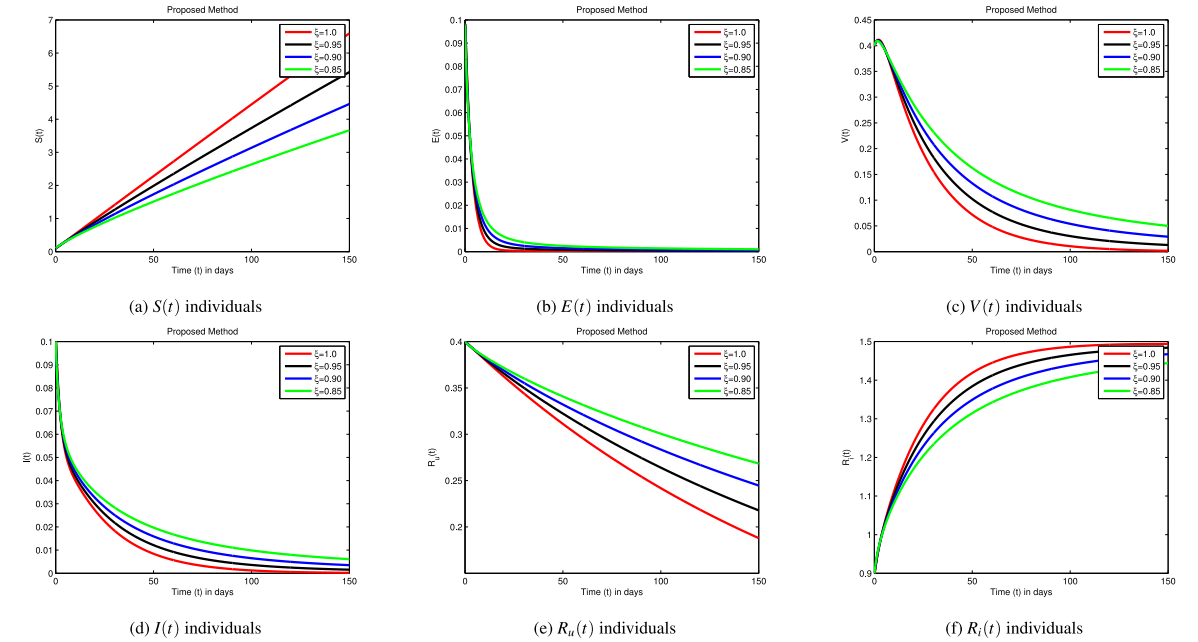

(a) $S(t)$ individuals (b) $E(t)$ individuals (c) $V(t)$ individuals

(d) $I(t)$ individuals (e) $R_u(t)$ individuals (f) $R_i(t)$ individuals

Fig. 5. Using ABC operator at different fractional values.

Similarly, we get expressions for $E(t)-E(0)$, $V(t)-V(0)$, $I(t)-I(0)$, $R_u(t)-R_u(0)$, and $R_i(t)-R_i(0)$.

Let $t=t_{n+1}$ for $n=0,1,2,\ldots$. The equations are reformulated as:

$$S(t_{n+1})-S(0)=\frac{(1-\xi)}{ABC(\xi)}f_1(t_n,S(t_n),G(t_n)) + \frac{\xi}{ABC(\xi)\Gamma(\xi)}\sum_{k=0}^{n}\int_{t_k}^{t_{k+1}} f_1(\sigma,S(\sigma),G(\sigma))(t_{n+1}-\sigma)^{\xi-1}d\sigma, \tag{10}$$

where $G(t_n)=(E(t_n),V(t_n),I(t_n),R_u(t_n),R_i(t_n))$.

Similarly, we get expressions for $E(t_{n+1})-E(0)$, $V(t_{n+1})-V(0)$, $I(t_{n+1})-I(0)$, $R_u(t_{n+1})-R_u(0)$, and $R_i(t_{n+1})-R_i(0)$.

Using two-step Lagrange polynomial interpolation within the interval $[t_k,t_{k+1}]$, we can simplify Eq. (10) to:

$$\begin{aligned}S_{n+1} &= S_0+\frac{(1-\xi)}{ABC(\xi)}f_1(t_n,S(t_n),G(t_n)) \\ &+\frac{\xi}{ABC(\xi)\Gamma(\xi)}\sum_{k=0}^{n}\left(\frac{f_1(t_k,S_k,G_k)}{h}\int_{t_k}^{t_{k+1}}(\sigma-t_{k-1})(t_{n+1}-\sigma)^{\xi-1}d\sigma\right. \\ &\left.-\frac{f_1(t_{k-1},S_{k-1},G_{k-1})}{h}\int_{t_k}^{t_{k+1}}(\sigma-t_k)(t_{n+1}-\sigma)^{\xi-1}d\sigma\right),\end{aligned} \tag{11}$$

where $G(t_k)=(E(t_k),V(t_k),I(t_k),R_u(t_k),R_i(t_k))$ and $G(t_{k-1})=(E(t_{k-1}),V(t_{k-1}),I(t_{k-1}),R_u(t_{k-1}),R_i(t_{k-1}))$.

Similarly, we get expressions for E_{n+1}, V_{n+1}, I_{n+1}, $R_{u_{n+1}}$, and $R_{i_{n+1}}$.

After integrating the terms, we replace them in Eq. (11) to get:

$$\begin{aligned}S_{n+1} &= S_0+\frac{(1-\xi)}{ABC(\xi)}f_1(t_n,S(t_n),G(t_n)) \\ &+\frac{\xi}{ABC(\xi)}\sum_{k=0}^{n}\left(\frac{h^\xi f_1(S_k,G_k)}{\Gamma(\xi+2)}\left((n+1-k)^\xi(n-k+2+\xi)\right.\right. \\ &\left.-(n-k)^\xi(n-k+2+2\xi)\right) \\ &\left.-\frac{h^\xi f_1(t_{k-1},S_{k-1},G_{k-1})}{\Gamma(\xi+2)}((n+1-k)^{\xi+1}-(n-k)^\xi(n-k+1+\xi))\right),\end{aligned}$$

Similarly, we get expressions for E_{n+1}, V_{n+1}, I_{n+1}, $R_{u_{n+1}}$, and $R_{i_{n+1}}$.

6. Simulation explanation

Theoretical results are obtained and examined using advanced approaches. Through simulations, the newly developed system is analyzed. The conjunctivitis model provides intriguing results using non-integer parametric values. Lowering fractional values yields reliable results for $S(t),E(t),V(t),I(t),R_u(t)$, and $R_i(t)$, as shown in Fig. 5.

Sub-figures (a) and (f) illustrate the dynamics of susceptible $S(t)$ and recovered with treatment $R_i(t)$, respectively. Both compartments increase rapidly and then stabilize. Sub-figures (b), (c), (d), and (e) show the dynamics of exposed $E(t)$, vaccinated $V(t)$, infected $I(t)$, and recovered without treatment $R_u(t)$. Each compartment declines dramatically before stabilizing.

Sub-figures (c), (d), and (e) demonstrate a significant drop in infections due to combined vaccination and treatment strategies. Recovery with and without medication increases as fractional values decrease, as seen in the sub-figures (e) and (f).

These findings suggest future research directions for preventing the spread of conjunctivitis. The Atangana–Toufik method yields superior results for all sub-compartments at fractional derivatives compared to conventional derivatives. Reducing fractional values improves the accuracy and reliability of solutions across all compartments.

7. Conclusion

In this article, we formulated a fractional order conjunctivitis virus model, incorporating vaccination and recovery measures with and without medication. Using the Atangana–Toufik technique, we analyzed the model to produce reliable results. We recommend vaccinations and immune-boosting measures to prevent the spread of the virus, promoting a disease-free environment. The model examines the global impact of conjunctivitis with and without treatment and uses bifurcation analysis to ensure stability. Our findings confirm that the model does not exhibit flip bifurcation, and the unique and bounded solutions are validated using Banach space results. Calculating the reproductive number R_0 is crucial for understanding epidemic potential. Sensitivity analysis highlights the most significant factors affecting disease transmission. MATLAB simulations illustrate the dynamics of conjunctivitis control, demonstrating that combined measures vaccination and hand hygiene can control the virus without medication. These findings support future research in early detection and understanding the virus's behavior and spread.

CRediT authorship contribution statement

Muhammad Owais Kulachi: Writing – original draft, Data curation, Conceptualization. **Aqeel Ahmad:** Writing – original draft, Validation, Supervision, Methodology. **Evren Hincal:** Writing – review & editing, Resources, Investigation, Funding acquisition. **Ali Hasan Ali:** Writing – review & editing, Visualization, Software, Project administration. **Muhammad Farman:** Writing – original draft, Investigation, Formal analysis, Conceptualization. **Muhammad Taimoor:** Writing – review & editing, Validation, Methodology, Conceptualization.

Declaration of competing interest

The authors declare that they have no known competing financial interests or personal relationships that could have appeared to influence the work reported in this paper.

References

Ahmad, A., Kulachi, M.O., Farman, M., Junjua, M.U.D., Bilal Riaz, M., Riaz, S., 2024. Mathematical modeling and control of lung cancer with IL 2 cytokine and anti-PD-L1 inhibitor effects for low immune individuals. PLoS One 19 (3), e0299560.

Alalhareth, F.K., Atta, U., Ali, A.H., Ahmad, A., Alharbi, M.H., 2023. Analysis of leptospirosis transmission dynamics with environmental effects and bifurcation using fractional-order derivative. Alex. Eng. J. 80, 372–382.

Alsaud, H., Kulachi, M.O., Ahmad, A., Taimoor, M., 2024. Investigation of SEIR model with vaccinated effects using sustainable fractional approach for low immune individuals. AIMS Math. 9 (4), 10208–10234.

Atangana, A., Baleanu, D., 2016. New fractional derivatives with nonlocal and non-singular kernel: Theory and application to heat transfer model. pp. 763–769, arXiv preprint arXiv:1602.03408.

Center for Disease Control (CDC), 0000. Conjunctivitis (pink eye). https://www.cdc.gov.

Chadha, N.M., Tomar, S., Raut, S., 2023. Parametric analysis of dust ion acoustic waves in superthermal plasmas through non-autonomous KdV framework. Commun. Nonlinear Sci. Numer. Simul. 123, 107269.

Chansaenroj, J., Vongpunsawad, S., Puenpa, J., Theamboonlers, A., Vuthitanachot, V., Chattakul, P., et al., 2015. Epidemic outbreak of acute haemorrhagic conjunctivitis caused by coxsackievirus A24 in Thailand, 2014. Epidemiol. Infect. 143 (14), 3087–3093.

Chou, C.S., Friedman, A., 2016. Introduction to Mathematical Biology: Modeling, Analysis, and Simulations. Springer.

Chowell, G., Shim, E., Brauer, F., Diaz-Duenas, P., Hyman, J.M., Castillo-Chavez, C., 2006. Modelling the transmission dynamics of acute haemorrhagic conjunctivitis: Application to the 2003 outbreak in Mexico. Stat. Med. 25 (11), 1840–1857.

Dayan, F., Ahmed, N., Ali, A.H., Rafiq, M., Raza, A., 2023. Numerical investigation of a typhoid disease model in fuzzy environment. Sci. Rep. 13 (1), 21993.

Elliot, R.H., 1925. Conjunctivitis in the tropics. Br. Med. J. 1 (3340), 12–14.

Fehily, S.R., Cross, G.B., Fuller, A.J., 2015. Bilateral conjunctivitis in a returned traveller. PLoS Negl. Trop. Dis. 9 (1), e0003351.

Ghazali, O., Chua, K.B., Ng, K.P., Hooi, P.S., Pallansch, M.A., Oberste, M.S., et al., 2003. An outbreak of acute haemorrhagic conjunctivitis in Melaka. Singapore Med. J. 44 (10), 511–516.

Kimberlin, D.W., 2018. Red Book: 2018-2021 Report of the Committee on Infectious Diseases (No. Ed. 31). American Academy of Pediatrics.

Kyere, S.N., Boateng, F.A., Hoggar, G.F., Jonathan, P., 2018. Optimal control model of haemorrhagic conjunctivitis disease. Adv. Comput. Sci. 1 (2), 108.

Malu, K.N., 2014. Allergic conjunctivitis in Jos-Nigeria. Niger. Med. J.: J. Niger. Med. Assoc. 55 (2), 166–170.

Murray, J.D., 2003. Mathematical Biology I. Springer Verlag Berlin Heidelbery.

Ngoma, H.D., Kiogora, P.R., Chepkwony, I., 2022. A fractional order model of leptospirosis transmission dynamics with environmental compartment. Glob. J. Pure Appl. Math. 18 (1), 81–110.

Sangsawang, S., Tanutpanit, T., Mumtong, W., Pongsumpun, P., 2012. Local stability analysis of mathematical model for hemorrhagic conjunctivitis disease. Curr. Appl. Sci. Technol. 12 (2), 189–197.

Sangthongjeen, S., Sudchumnong, A., Naowarat, S., 2015. Effect of educationa campaign on tranmission model of conjunctivitis. Aust. J. Basic Appl. Sci. 9 (7), 811–815.

Suksawat, J., Naowarat, S., 2014. Effect of rainfall on the transmission model of conjunctivitis. Adv. Environ. Biol. 8 (14), 99–104.

Tomar, S., Chadha, N.M., 2023. Study of fixed points and chaos in wave propagation for the generalized damped forced Korteweg-de Vries equation using bifurcation analysis. Chaos Theory Appl. 5 (4), 286–292.

Tomar, S., Chadha, N.M., Khanna, A., 2023. A mathematical model to study regulatory properties and dynamical behaviour of glycolytic pathway using bifurcation analysis. In: Computational Methods for Biological Models. Springer Nature Singapore, Singapore, pp. 81–116.

Unyong, B., Naowarat, S., 2014. Stability analysis of conjunctivitis model with nonlinear incidence term. Aust. J. Basic Appl. Sci. 8 (24), 52–58.

Yeargers, E.K., Herod, J.V., Shonkweiler, R.W., 2013. An Introduction To the Mathematics of Biology: With Computer Algebra Models. Springer Science & Business Media.